Chinese Chemical Letters 31 (2020) 3139–3142

Contents lists available at ScienceDirect

Chinese Chemical Letters

journal homepage: www.elsevier.com/locate/cclet

Communication

Cationic and temperature-sensitive liposomes loaded with eugenol for the application to silk

Zhiguo Lu[a,c], Xiangyu Wang[a], Tianlu Zhang[a,c], Luyao Zhang[a,c], Jun Yang[a], Yan Li[a], Jie Shen[a,c], Jianze Wang[a], Yunwei Niu[d,e], Zuobing Xiao[d,e], Guiying Liu[b,*], Xin Zhang[a,*]

[a] State Key Laboratory of Biochemical Engineering, Institute of Process Engineering, Chinese Academy of Sciences, Beijing 100190, China
[b] Department of Pediatrics, Capital Medical University Affiliated Beijing Anzhen Hospital, Beijing 100029, China
[c] School of Chemical Engineering, University of Chinese Academy of Sciences, Beijing 100049, China
[d] Shanghai Research Institute of Fragrance and Flavor Industry, Shanghai 200232, China
[e] School of Perfume and Aroma Technology, Shanghai Institute of Technology, Shanghai 200233, China

ARTICLE INFO

Article history:
Received 11 May 2020
Received in revised form 6 July 2020
Accepted 6 July 2020
Available online 7 July 2020

Keywords:
Eugenol
Silk
Cationic and temperature-sensitive liposomes
Slow release of fragrance
Controlled release of fragrance

ABSTRACT

Silk has been widely used in the clothing industry due to their soft and smooth features, good biocompatibility, good heat dissipation, warmth and ultraviolet resistance. The application of fragrance to silk can significantly improve the performance of silk. However, there are two key scientific problems that need to be solved: slowing down the release rate of fragrances and increasing the scent lasting time of silk. In this study, cationic and temperature-sensitive liposomes were designed and prepared to encapsulate eugenol. These fragrance-loaded liposomes significantly slowed down the release rate of the fragrance and controlled the release rate of the fragrance in a thermo-sensitive manner. The liposomes adhered to the silk through electrostatic adsorption interaction. The positive charge on the fragrance-loaded liposomes neutralized much negative charge on silk and thereby increasing the adhesion efficiency.

Silk is a textile composed of silk fibroin, so it has good biocompatibility [1–3]. In addition, silk is soft and smooth. The friction coefficient of silk on the human body is the lowest among all types of fibers. Furthermore, silk also has good heat dissipation, warmth and ultraviolet resistance. Therefore, silk is widely used in the clothing industry.

With the development of the fine chemical industry, fragrances are widely used in daily life [4–7]. Adding fragrances to silk can significantly improve the performance of silk. However, the fragrance is highly volatile, which causes the fragrances to be released from the silk quickly [8,9]. On the one hand, this leads to an excessively strong aroma, which affects the user experience. On the other hand, this also leads to a short scent lasting time. Therefore, slowing down the release rate of fragrances and increasing the scent lasting time of silk are the key scientific problems that need to be solved if fragrances are applied to silk.

Nanoscience and nanotechnology are widely used in the encapsulation, delivery, sustained release and controlled release of drugs. Cationic nanoparticles can adsorb anionic drugs, such as DNA and proteins, by electrostatic interaction [10–12]. Mesoporous nanomaterials can adsorb small molecule drugs and release the drugs slowly due to their large surface tension [13–17]. Many nanomaterials are combined with drugs to form prodrugs, thereby achieving sustained and controlled release of drugs [18–22]. The micelles and liposomes based on the hydrophilic-hydrophobic interaction can encapsulate the drugs and achieve slow and controlled release of the drugs [23–27]. These nanomaterials have the potential to encapsulate fragrances and release fragrances slowly. There are two problems to be solved to prolong the scent lasting time of silk. Firstly, the fragrances are released from nanomaterials controllably. That is, when using silk, the nanomaterials promote the release of fragrance. When silk is not used, the release of fragrance is inhibited. Secondly, the adhesion of nanomaterials to silk needs to be strong.

Since silk is mainly composed of silk fibroin, the surface potential of silk is negative. In addition, silk is mainly used close to the body. In this study, cationic and temperature-sensitive liposomes were designed and prepared to encapsulate eugenol based on these two characteristics of silk. As shown in Fig. 1, the cationic and temperature-sensitive polymer poly[*N*-isopropylacrylamide-*co*-2-(dimethylamino)ethyl acrylate-phenylboronic acid] (p(NIPAM-*co*-DMAEA-PBA)) was synthesized. The lipid

* Corresponding authors.
E-mail addresses: liugvying@126.com (G. Liu), xzhang@ipe.ac.cn (X. Zhang).

https://doi.org/10.1016/j.cclet.2020.07.013
1001-8417/

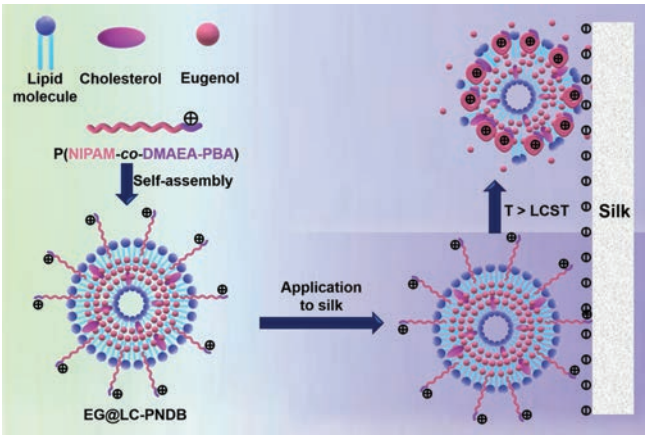

Fig. 1. The schematic diagrams of the preparation of EG@LC-PNDB, the application of EG@LC-PNDB to silk and the control release of eugenol.

molecules, p(NIPAM-*co*-DMAEA-BPA), cholesterol and eugenol were self-assembled. The fragrance-loaded liposomes were named EG@LC-PNDB. The EG@LC-PNDB adhered to silk by electrostatic interaction. When the temperature was higher than the low critical phase transition temperature (LCST), p(NIPAM-*co*-DMAEA-PBA) shrinks. This disrupted the structure of EG@LC-PNDB, thereby promoting the release of fragrance molecules.

N-Isopropylacrylamide (NIPAM, 98%), 2-(dimethylamino)ethyl acrylate (DMAEA, 98%), 4-(bromomethyl)phenylboronic acid (PBA, 98%), 2-aminoethanethiol (AET, 97%), 2,2′-azoisobutyronitrile (AIBN, 99%) and cholesterol (95%) were purchased from J&K Scientific. 1,2-Distearoyl-*sn*-glycero-3-phosphoethanolamine-N-[(polyethylene glycol)-2000] (DSPE-PEG2000), 1,2-dipalmitoyl-*sn*-glycero-3-phosphocholine (DPPC) and L-aphosphatidylcholine(soy-hydrogenated) (HSPC) were purchased from A.V.T. (Shanghai) Pharmaceutical Co., Ltd. Methanol, hexane, *N*,*N*-dimethylformamide (DMF) and chloroform were purchased from Sinopharm Chemical Reagent Co., Ltd. And these chemicals were all of analytical grade and used without further purification.

p(NIPAM-*co*-DMAEA-PBA) with three molar ratios of NIPAM to DMAEA-PBA (90:10, 80:20 and 70:30) were synthesized. When the molar ratio of NIPAM to DMAEA-PBA was 90:10, the synthesis method was as follows. DMAEA (141.5 mg), NIPAM (1018.4 mg), AET (14.77 mg) and AIBN (6.95 mg) were dissolved into methanol and then putted into a Schlenk bottle. The system was degassed by freeze-pump-thaw cycles and recharged with N_2 for three times. The reaction was then heated at 65 °C for 24 h under stirring. The reaction solution was then carried into ice cold hexane. The precipitate was collected by filtration and then dried under vacuum for 24 h to obtain p(NIPAM-*co*-DMAEA). The p(NIPAM-*co*-DMAEA) was characterized by ^{1}H NMR on a Bruker 600 MHz spectrometer. The p(NIPAM-*co*-DMAEA) and PBA were dissolved in DMF at room temperature for 24 h to synthesize PNIPAM-BMAEA. The product was purified by dialysis against methanol and deionized water. The dialysate was then lyophilized to obtain p(NIPAM-*co*-DMAEA-PBA). The p(NIPAM-*co*-DMAEA-PBA) was characterized by ^{1}H NMR on a Bruker 600 MHz spectrometer. The LCST was measured by a differential scanning calorimetry (DSC).

The lipid molecules (DPPC and HSPC), cholesterol, p(NIPAM-*co*-DMAEA-PBA) and eugenol were dissolved in chloroform and mixed uniformly. The solvent was then removed on a rotary evaporator at 37 °C. The solutes formed a thin lipid film. The solutes were under vacuum to remove residual chloroform. In the following, the lipid film was hydrated in deionized water under ultrasonic condition for 30 min to obtain the eugenol-loaded liposomes (EG@LC-PNDB).

The preparation method of EG@LC-PEG is similar to that of EG@LC-PNDB. In brief, DPPC, HSPC, cholesterol, DSPE-PEG2000 and eugenol were dissolved in chloroform and mixed uniformly. Chloroform was then removed on a rotary evaporator at 37 °C and the solutes formed a thin lipid film. The residual chloroform was then removed under vacuum. The lipid film was hydrated in deionized water under ultrasonic condition for 30 min to obtain EG@LC-PEG.

The average size and zeta potential of EG@LC-PNDB were measured by dynamic light scattering (DLS). The morphology of EG@LC-PNDB was observed by transmission electron microscope (TEM). The encapsulation efficiency of EG@LC-PNDB was measured by an ultraviolet-visible spectrophotometer (UV–vis) at 278 nm wavelength.

The EG@LC-PNDB was carried into a dialysis bag (MWCO 3500) and incubated in deionized water at different temperature under horizontal shaking (150 rpm). At predetermined time intervals, deionized water (0.5 mL) was removed to be detected and fresh deionized water (0.5 mL) was added. The concentration of eugenol in the removed deionized water was measured by a UV–vis at 278 nm wavelength. The release of eugenol was calculated by the formula: Eugenol release (%) = $W_1/W_2 \times 100\%$, where W_1 is the weight of eugenol in the deionized water, W_2 is the weight of total eugenol in the EG@LC-PNDB.

The silk was soaked in the EG@LC-PNDB at room temperature for 12 h and then was dried at 50 °C for 30 min. The surface potentials of untreated silk and EG@LC-PNDB-treated silk were measured by an electrokinetic analyzer for solid surface analysis: SurPASS^{TM} 3 (Anton Paar, Austria). The adhension efficiency of eugenol in silk was measured by a UV–vis. Briefly, the EG@LC-PNDB-treated silk was soaked in methanol under ultrasonic condition for 30 min. The concentration of eugenol in the methanol was measured by a UV–vis at 278 nm wavelength. In the statistical analysis, all data were expressed as mean ± SD unless otherwise indicated, and statistical significance was analyzed using one-way ANOVA.

The synthetic route of p(NIPAM-*co*-DMAEA-PBA) was shown in Fig. 2A. Firstly, p(NIPAM-*co*-DMAEA) was synthesized by a polymerization reaction. The PDMAEA was thermo-sensitive block and shrank when the temperature was higher than the LCST. Secondly, p(NIPAM-*co*-DMAEA-PBA) was synthesized by an addition reaction. There were quaternary amine groups at the block of p(DMAEA-PBA), so the p(DMAEA-PBA) was cationic block. The LCST and electropositivity were the most important indicators of p(NIPAM-*co*-DMAEA-PBA). These two indicators were stated with the molar ratio of NIPAM to DMAEA-PBA. So, p(NIPAM-*co*-DMAEA-PBA) with three molar ratios of NIPAM to DMAEA-PBA (90:10, 80:20 and 70:30) were synthesized. Fig. 2B showed the ^{1}H NMR spectra of p(NIPAM-*co*-DMAEA), which proved the successful synthesis of p(NIPAM-*co*-DMAEA). Fig. 2C showed the ^{1}H NMR spectra of p(NIPAM-*co*-DMAEA-PBA). The chemical shifts at 7.32 ppm and 7.60 ppm was caused by the benzene ring at PBA, which indicated the successful synthesis of p(NIPAM-*co*-DMAEA-PBA).

The LCSTs of p(NIPAM-*co*-DMAEA-PBA) with different molar ratios of NIPAM to DMAEA-PBA were then measured by DSC. As shown in Fig. 3A, as the molar ratio of NIPAM to DMAEA-PBA decreased, the LCST of p(NIPAM-*co*-DMAEA-PBA) increased. The p(NIPAM-*co*-DMAEA-PBA) needed to change the phase when the silk was used, and it could not change the phase when the silk was not used. Besides, the silk usually touched the body when it was used, and placed in the room when it was not used. Therefore, the LCST of p(NIPAM-*co*-DMAEA-PBA) should be between room temperature and human body temperature. P(NIPAM-co-DMAEA-PBA) with molar ratio of NIPAM to DMAEA-PBA was 100:0 and 90:10 was eligible and the LCSTs were 33.5 °C and

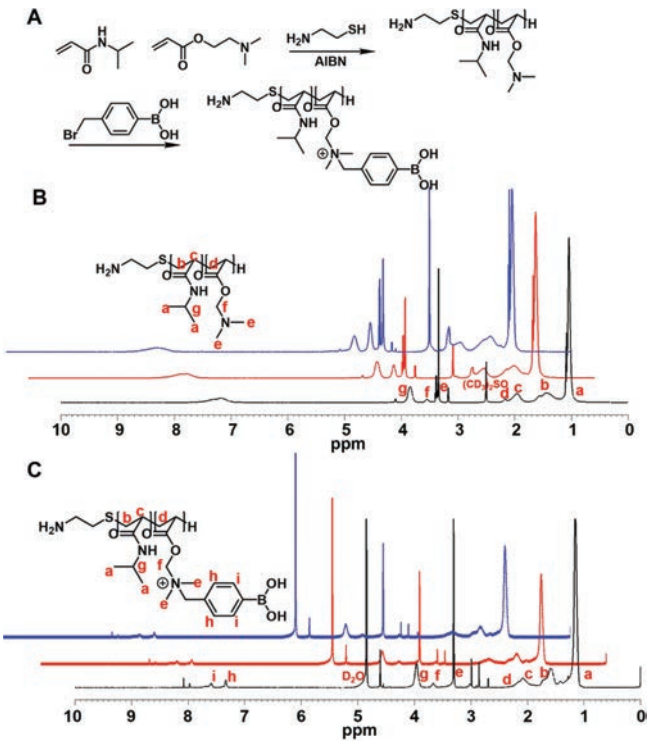

Fig. 2. (A) The synthetic route of p(NIPAM-*co*-DMAEA-PBA). (B) The ^{1}H NMR spectra of p(NIPAM-*co*-DMAEA). The red, blue and black lines represented molar ratios of NIPAM to DMAEA of 90:10, 80:20 and 70:30, respectively. (C) The ^{1}H NMR spectra of p(NIPAM-*co*-DMAEA-PBA). The red, blue and black lines represented molar ratios of NIPAM to DMAEA-PBA of 90:10, 80:20 and 70:30, respectively.

35.8 °C, respectively. When the proportion of DMAEA-PBA increased, the cationic quaternary ammoniums increased. Therefore, p(NIPAM-co-DMAEA-PBA) with a molar ratio of 90:10 was chosen to encapsulate eugenol. In order to explore the effects of p (NIPAM-*co*-DMAEA-PBA), DSPE-PEG2000 was chosen to replace the p(NIPAM-*co*-DMAEA-PBA) and the fragrance-loaded liposome was named EG@LC-PEG. The blank carriers were named LC-PDNB and LC-PEG, respectively. The hydrodynamic diameters of LC-PDNB, EG@LC-PDNB, LC-PEG and EG@LC-PEG were measured by DLS. As shown in Fig. 3B, the average diameters of LC-PDNB, EG@LC-PDNB, LC-PEG and EG@LC-PEG were 318.8, 342.0, 214.8 and 220.2 nm, respectively. The zeta potentials of LC-PDNB, EG@LC-PDNB, LC-PEG and EG@LC-PEG were also detected by DLS. As shown in Fig. 3C, the zeta potential of LC-PDNB and EG@LC-PDNB reached 45.2 mV and 43.0 mV, respectively. By contrast, the zeta potential of LC-PEG and EG@LC-PEG was –4.8 mV and –4.0 mV. That was, EG@LC-PEG was anionic liposome, which might be due to the large number of phospholipids in the EG@LC-PEG. The morphology of EG@LC-PDNB was observed by TEM. As shown in Fig. 3D, the EG@LC-PDNB was spherical and the diameter was about 200 nm, which was small than the hydrodynamic diameter that measured by DLS. This might be due to the hydration of the liposome.

In the following, the encapsulation efficiencies of the eugenol-loaded liposomes were measured by a UV–vis. As shown in Fig. 4A, the encapsulation efficiency of EG@LC-PDNB was 35.0%, which was 1.46 times that of encapsulation efficiency of EG@LC-PEG. The release profiles of eugenol were shown in Fig. 4B. After 3 h, 78.6% of free eugenol was released and nearly 90% of free fragrance was released after 12 h. By contrast, after 144 h (7 days), less than 30% of fragrance was released from the eugenol-loaded liposomes. This result showed that liposomes could slow the release rate of eugenol. At 25 °C and 37 °C, the release profiles of eugenol from EG@LC-PEG were almost the same. This result indicated that EG@LC-PEG did not controllably release fragrance in a thermo-sensitive manner. By contrast, the release rate of eugenol from EG@LC-PDNB at 37 °C was significantly faster than its release rate at 25 °C. 28.5% of eugenol was released from EG@LC-PDNB at 37 °C, which was 2.16 times that of the release percentage at 25 °C. This result proved the thermo-sensitive performance of EG@LC-PDNB. These results demonstrated that liposome could slow down the released rate of fragrance and p(NIPAM-*co*-DMAEA-PBA) contributed to the control release of fragrance in a thermo-sensitive manner. The surface potentials of different silks were then measured. As shown in Fig. 4C, the surface potential of untreated silk was –125.6 mV, which proved the strong negative charge on the surface of untreated silk. After attaching EG@LC-PEG, the surface potential of the silk was up to –129.4 mV, which was due to the negative charge on the EG@LC-PEG. By contrast, the surface potential of EG@LC-PDNB treated silk was only –35.4 mV. That was, much negative charge on the silk was neutralized by the positive charge of EG@LC-PDNB. The adhesion efficiency was shown in Fig. 4D. The adhesion efficiency of EG@LC-PDNB was up to 19.57%,

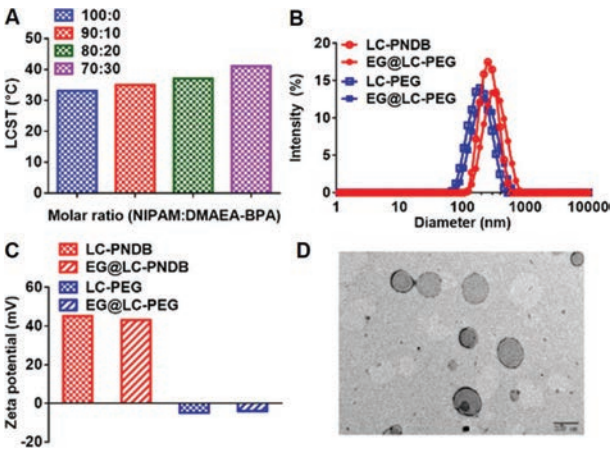

Fig. 3. (A) The LCST of p(NIPAM-*co*-DMAEA-PBA) with different molar ratios of NIPAM to DMAEA-PBA. (B) The hydrodynamic diameters of LC-PDNB, EG@LC-PDNB, LC-PEG and EG@LC-PEG. (C) The zeta potentials of LC-PDNB, EG@LC-PDNB, LC-PEG and EG@LC-PEG. (D) The TEM image of EG@LC-PDNB.

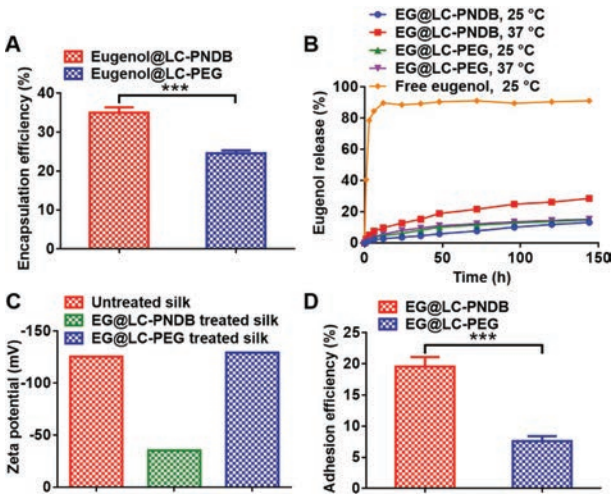

Fig. 4. (A) The encapsulation efficiencies of EG@LC-PDNB and EG@LC-PEG. (B) The release profiles of eugenol from different samples at different temperature. (C) The zeta potentials of untreated silk and eugenol treated silk. (D) The adhesion efficiencies of EG@LC-PDNB and EG@LC-PEG. Mean ± SD is shown ($n = 3$). ***$P <$ 0.005.

which was 2.57 times that of the adhesion efficiency of EG@LC-PEG. This might be caused by two reasons. Firstly, the encapsulation efficiency of EG@LC-PDNB was distinctly higher than the encapsulation efficiency of EG@LC-PEG. Secondly, the electrostatic interaction significantly improved the adsorption of EG@LC-PDNB on silk.

In summary, cationic and temperature-sensitive polymers p(NIPAM-*co*-DMAEA-PBA) was synthesized. The LCST of p(NIPAM-*co*-DMAEA-PBA) was 35.8 °C when the molar ratio of NIPAM to DMAEA-PBA was 90:10. Subsequently, liposomes based on p(NIPAM-*co*-DMAEA-PBA) were prepared to load eugenol and the liposomes were named EG@LC-PDNB. P(NIPAM-*co*-DMAEA-PBA) provided EG@LC-PDNB with much positive charge and increase the encapsulation efficiency of eugenol. Besides, the structures of liposomes significantly slow down the release rate of fragrance. P(NIPAM-*co*-DMAEA-PBA) contributed to the control release of fragrance in a thermo-sensitive manner. In the following, EG@LC-PDNB was added into the silk by electrostatic interaction and much negative charge on the silk was neutralized by the positive charge of EG@LC-PDNB. The electrostatic interaction between EG@LC-PDNB and silk obviously increased the adhesion efficiency. Therefore, cationic and temperature-sensitive EG@LC-PDNB could slow down the release rate of fragrances and increase the scent lasting time of silk.

Declaration of competing interest

The authors declare no conflict of interest.

Acknowledgments

This work was financially supported by the National High Technology Research and Development Program (No. 2016YFA0200303), the Beijing Natural Science Foundation (Nos. L172046, 2192057), the National Natural Science Foundation of China (Nos. 31771095, 21875254 and 51573188).

References

[1] J.A. Stinson, W.K. Raja, S. Lee, H. Bum, ACS Biomater. Sci. Eng. 3 (2017) 360–369.
[2] C. Yin, A.W. Jatoi, H. Bang, M. Gopiraman, I.S. Kim, Fiber. Polym. 17 (2016) 1140–1145.
[3] S. Wang, Y. Zhang, H. Wang, Z. Dong, Int. J. Biol. Macromol. 48 (2011) 345–353.
[4] F.G. Hougeir, L. Kircik, Dermatol Ther. 25 (2012) 234–237.
[5] I. van der Plancken, L. Verbeyst, K. de Vleeschouwer, et al., Trends Food Sci. Tech. 23 (2012) 28–38.
[6] M.B. Pashazanousi, M. Raeesi, S. Shirali, Asian J. Chem. 24 (2012) 4331–4334.
[7] N. Pazyar, R. Yaghoobi, N. Bagherani, A. Kazerouni, Int. J. Dermatol. 52 (2013) 784–790.
[8] A.M. Borda, D.G. Clark, D.J. Huber, B.A. Welt, T.A. Nell, Postharvest Biol. Tec. 59 (2011) 245–252.
[9] D.L. Berthier, I. Schmidt, W. Fieber, et al., Langmuir 26 (2010) 7953–7961.
[10] Z. Guo, S. Li, Z. Liu, W. Xue, ACS Biomater. Sci. Eng. 4 (2018) 988–996.
[11] J. Zhang, J. Cui, Y. Deng, Z. Jiang, W.M. Saltzman, ACS Biomater. Sci. Eng. 2 (2016) 2080–2089.
[12] Y. Yuan, F. Gong, Y. Cao, et al., J. Biomed. Nanotechnol. 11 (2015) 668–679.
[13] J. Shen, Z. Lu, T. Zhang, et al., J. Biomed. Nanotechnol. 14 (2018) 1556–1567.
[14] Y.H. Cui, R. Deng, X. Li, X. Wang, Y.W. Yang, Chin. Chem. Lett. 30 (2019) 2291–2294.
[15] V. Lebret, L. Raehm, J.O. Durand, M. Smaïhi, C. Dubernet, J. Biomed. Nanotechnol. 6 (2010) 176–180.
[16] A. Zhang, L. Hai, T. Wang, et al., Chin. Chem. Lett. (2020), doi:http://dx.doi.org/10.1016/j.cclet.2020.04.035.
[17] Y.J. Cheng, S.Y. Qin, Y. Ma, et al., ACS Biomater. Sci. Eng. 5 (2019) 1878–1886.
[18] D. Li, X. Feng, L. Chen, J. Ding, X. Chen, ACS Biomater. Sci. Eng. 4 (2018) 539–546.
[19] L. Qiu, L. Zhao, C. Xing, Y. Zhan, Chin. Chem. Lett. 29 (2018) 301–304.
[20] X. Jia, M. Pei, X. Zhao, et al., ACS Biomater. Sci. Eng. 2 (2016) 1641–1648.
[21] C. Chen, Y. Li, X. Yu, et al., Chin. Chem. Lett. 29 (2018) 1609–1612.
[22] M. Ni, W.J. Zeng, X. Xie, et al., Chin. Chem. Lett. 28 (2017) 1345–1351.
[23] R.M. Lopes, M.M. Gaspar, J. Pereira, C.V. Eleutério, M.E.M. Cruz, J. Biomed. Nanotechnol. 10 (2014) 3647–3657.
[24] Q. Hu, L. Bai, Z. Zhu, et al., Chin. Chem. Lett. 31 (2020) 915–918.
[25] V. Saxena, M.D. Hussain, J. Biomed. Nanotechnol. 9 (2013) 1146–1154.
[26] H. Li, J. Li, X. He, et al., Chin. Chem. Lett. 30 (2019) 1083–1088.
[27] J. Cao, S. Zhai, C. Li, et al., J. Biomed. Nanotechnol. 9 (2013) 1847–1861.